Supplement of Atmos. Meas. Tech., 12, 2611–2629, 2019
https://doi.org/10.5194/amt-12-2611-2019-supplement

Atmospheric Measurement Techniques
Open Access
EGU

Supplement of

A segmentation algorithm for characterizing rise and fall segments in seasonal cycles: an application to XCO_2 to estimate benchmarks and assess model bias

Leonardo Calle et al.

Correspondence to: Leonardo Calle (leonardo.calle@montana.edu)

Content Summary:

A series of figures are presented to extend the level of detail provided in the main text. The first Figure (S1) shows a standard multi-panel figure outputted by the segmentation algorithm. The second set of Figures (S2-S4) show the spatial coverage of the satellite retrievals by month. A multi-plot panel of seasonal cycles are shown in Figure S5 to clarify the influence of co-location sampling on deviations in otherwise Rise and Fall patterns in the seasonal cycle. The residuals of the seasonal cycle fit to GOSAT data are shown in Figure S6. For readers that are interested in the standard presentation of model bias in the form of Taylor diagrams, a panel of Taylor diagrams are provided for reference only in Figure S7. A sample comparison is provided in Figure S8 of seasonal cycle metrics derived using a mean seasonal cycle (no interannual variation) versus metrics derived from the seasonal cycle with interannual variation included. Figure S9 shows a plot of the long-term (2009-2012) linear growth rates, as this is an important pattern in the data that is not covered in detail in this study. Lastly, and for those readers that are interested, Figures S10-S13 show the correlation matrix for Northern and Southern Hemisphere regions, by Rise and Fall segments.

Figure S1. (a) Detrended XCO_2 seasonal cycles for the Europe TransCom region; (black line) GOSAT; (red line) CLM DGVM; (dashed line) fossil fuel; (dotted line) ocean. The DGVM (land) signal is clearly evident in the satellite derived seasonal cycle. Matching Rise segments between GOSAT and DGVM are highlighted in blue and close-up shown in (b); only a limited number of points are displayed for presentation. (c) The phase error for the matching segment represents the speed of the segment relative to the observed segment of the full signal; the time-series of the phase error is always linear. (d) The magnitude error represents the ability of the model to match the magnitude of the observed segment over time; the magnitude error is typically non-linear.

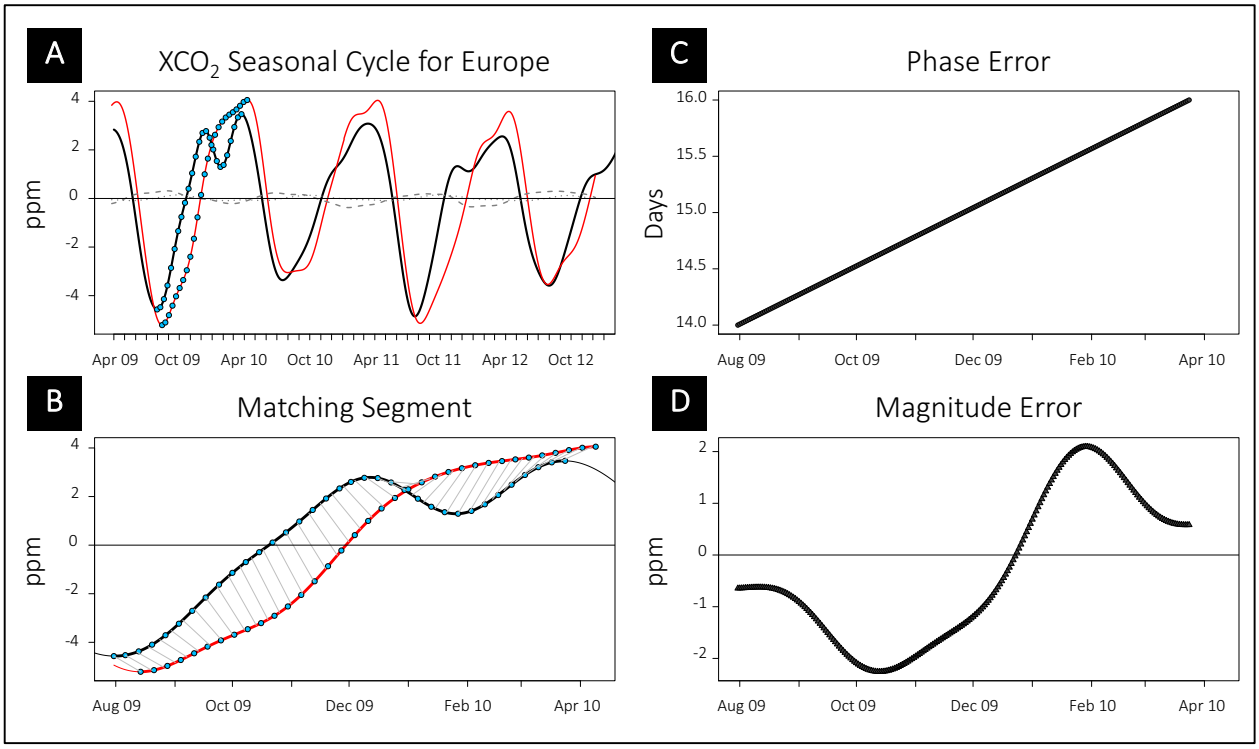

Figure S2. GOSAT retrievals for months of January - April, averaged for 2009-2014.

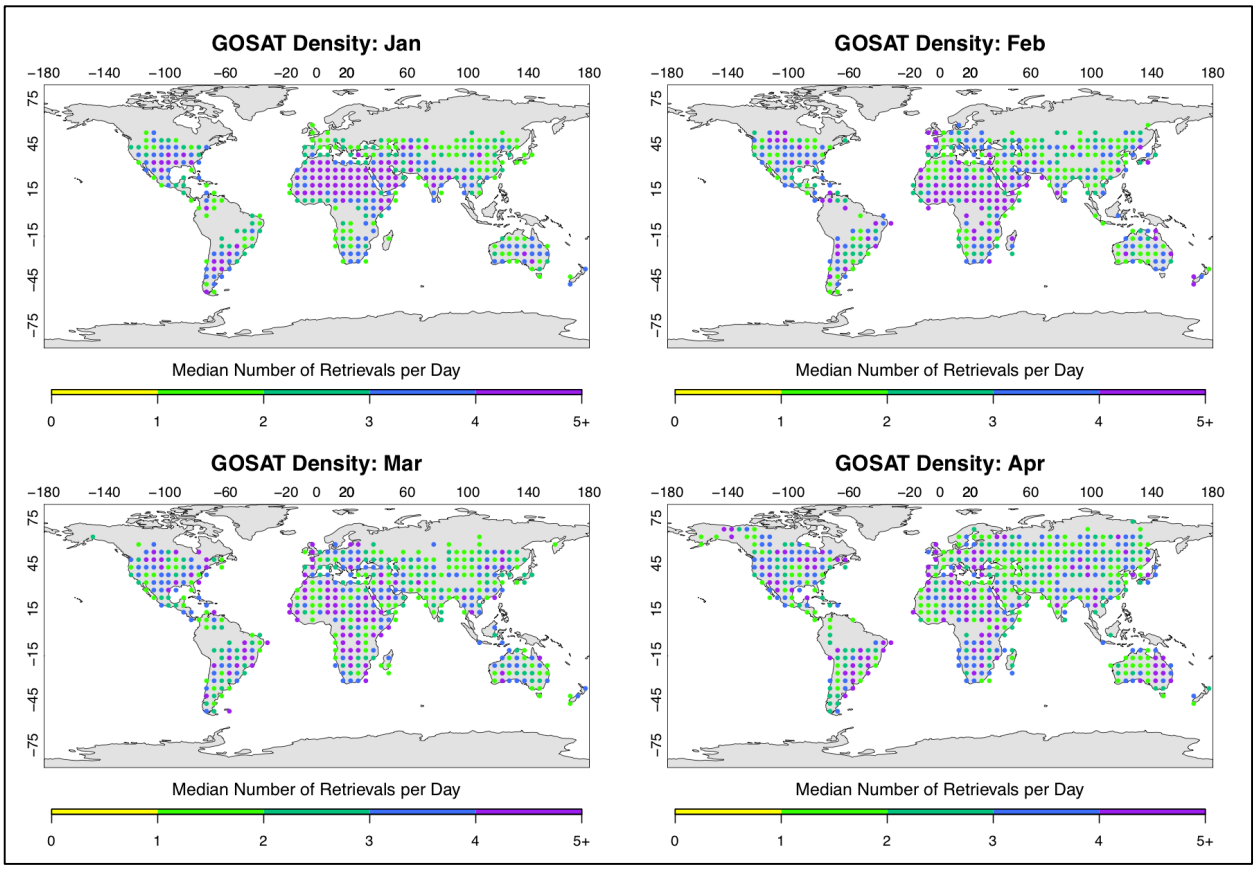

Figure S3. GOSAT retrievals for months of May - August, averaged for 2009-2014.

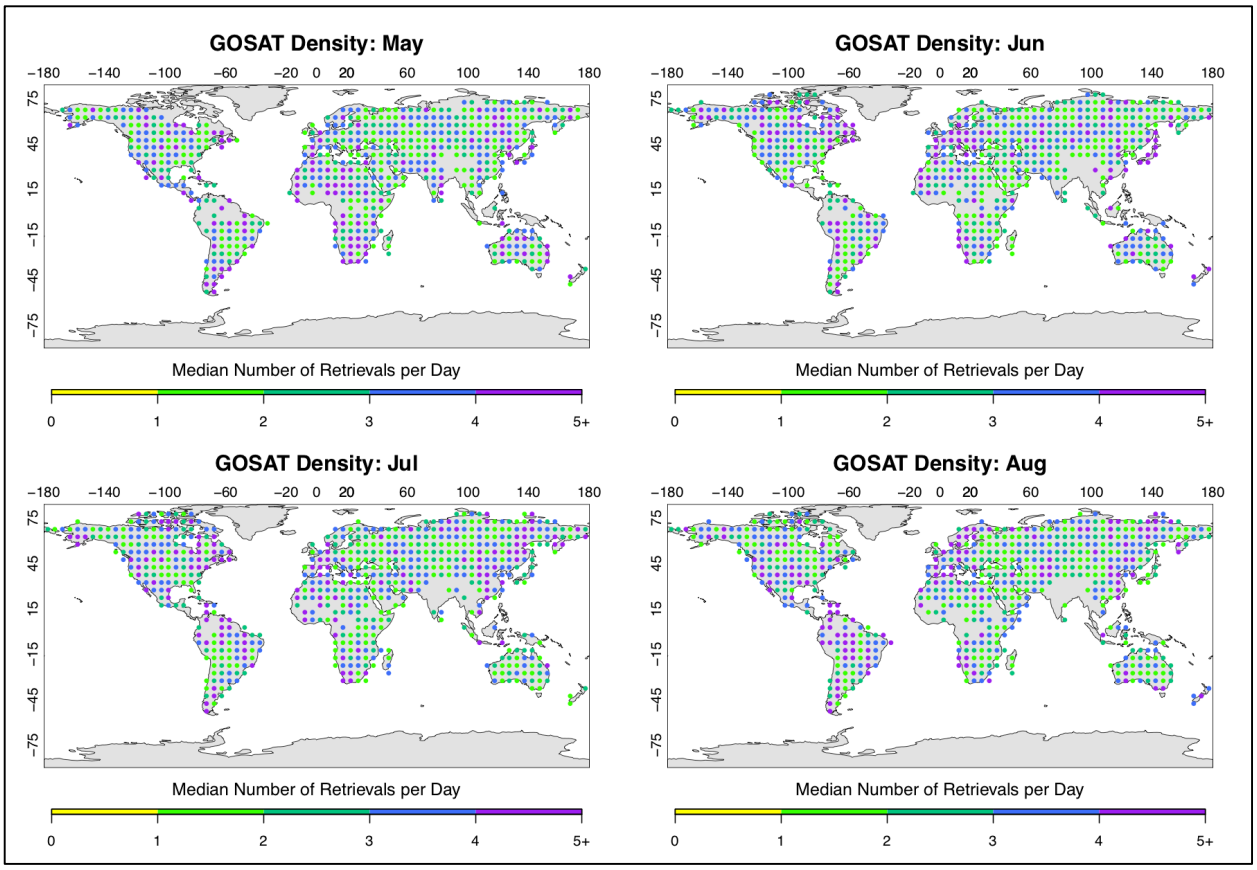

Figure S4. GOSAT retrievals for months of September - December, averaged for 2009-2014.

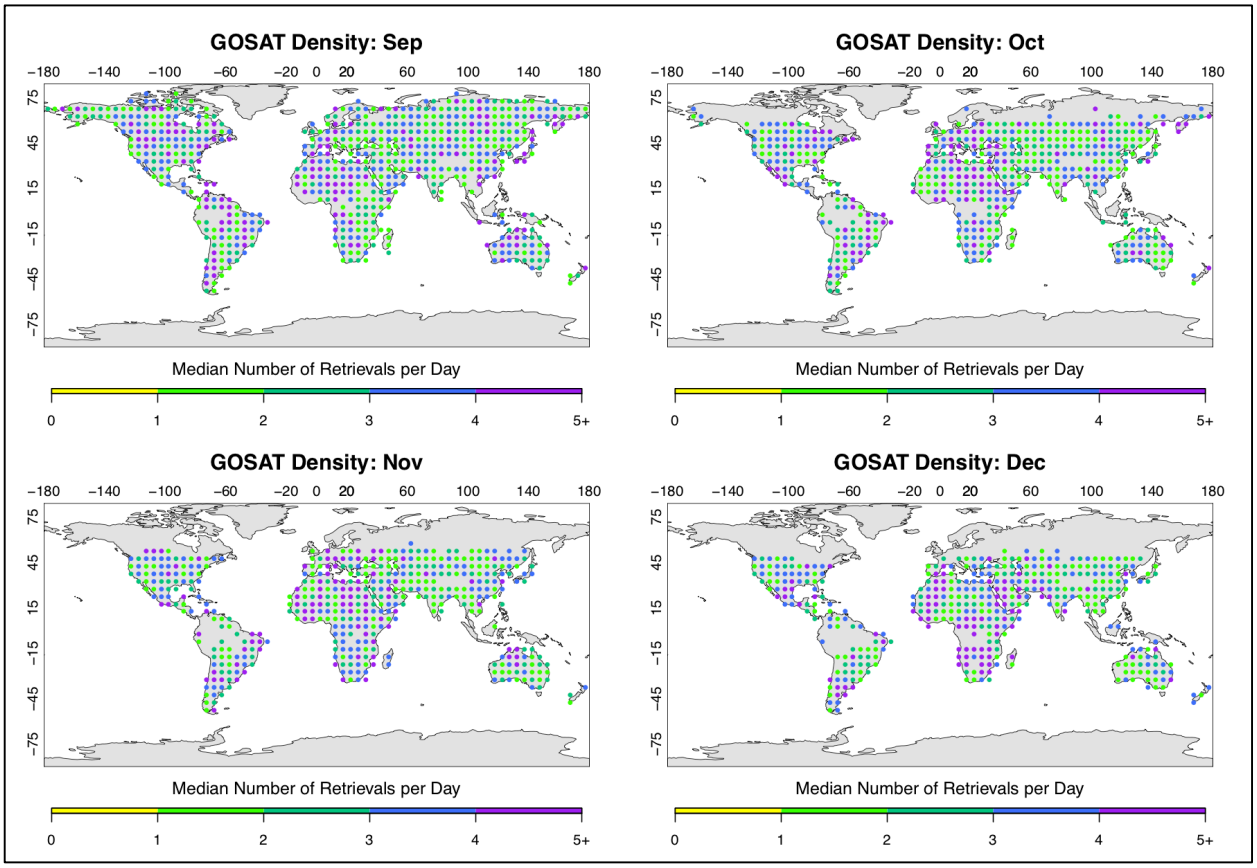

Figure S5. A comparison of seasonal cycles derived using complete coverage of simulated XCO_2 data (red lines) versus co-location sampling (blue lines) to match time and spatial location of GOSAT observations (black lines). The simulated seasonal cycles using all component fluxes of DGVM, fossil fuel, and ocean (solid lines) and that of the DGVM only (dashed line).

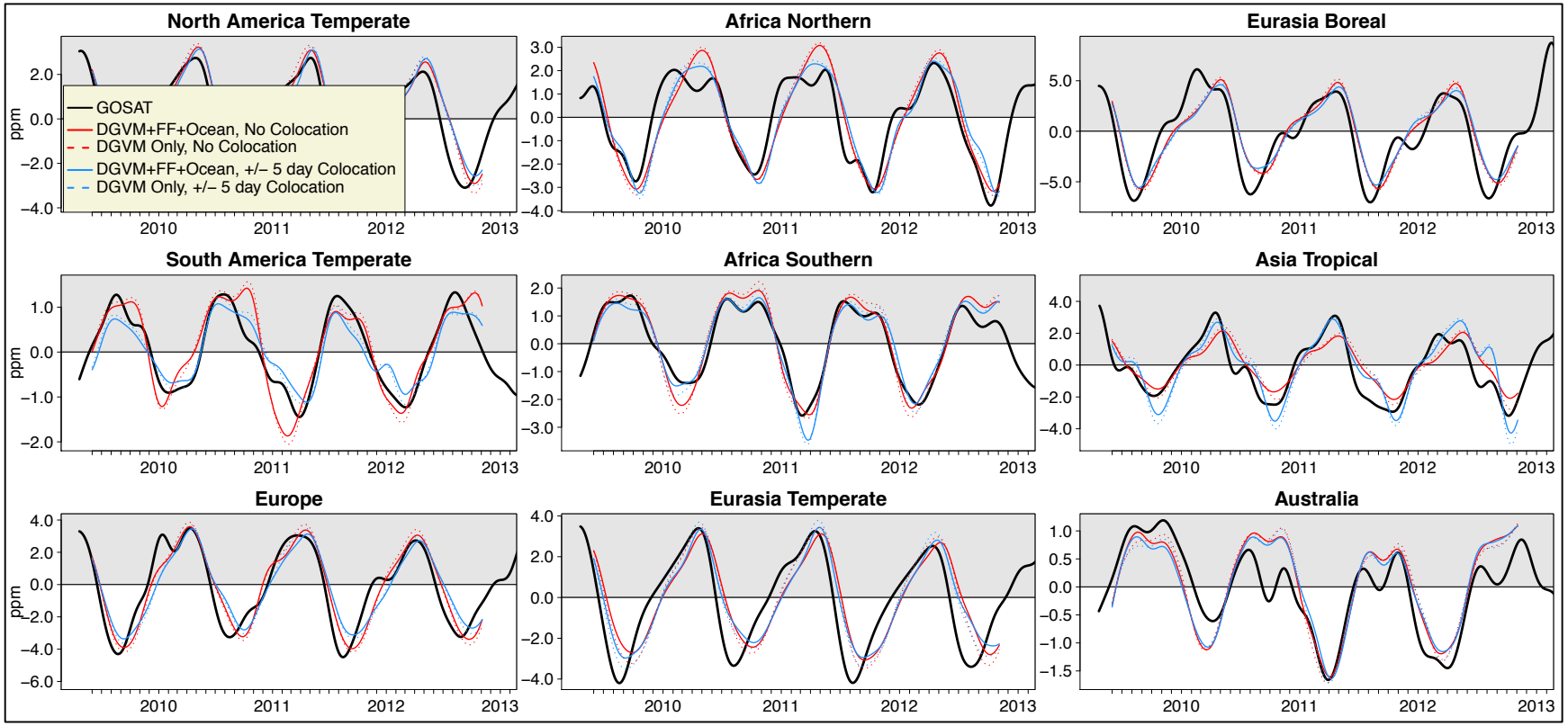

Figure S6. Seasonal cycle residuals for GOSAT.

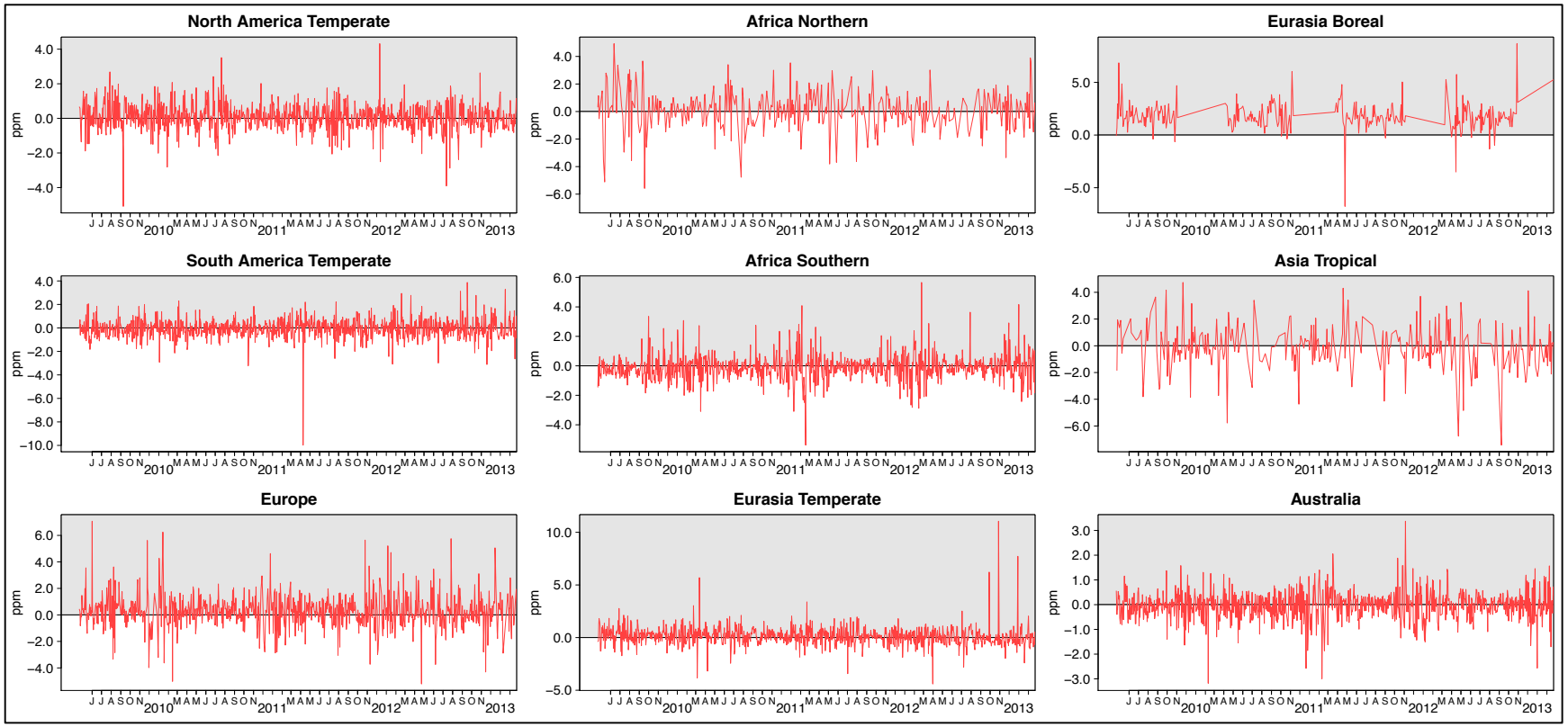

Figure S7. Taylor diagrams for all TransCom regions.

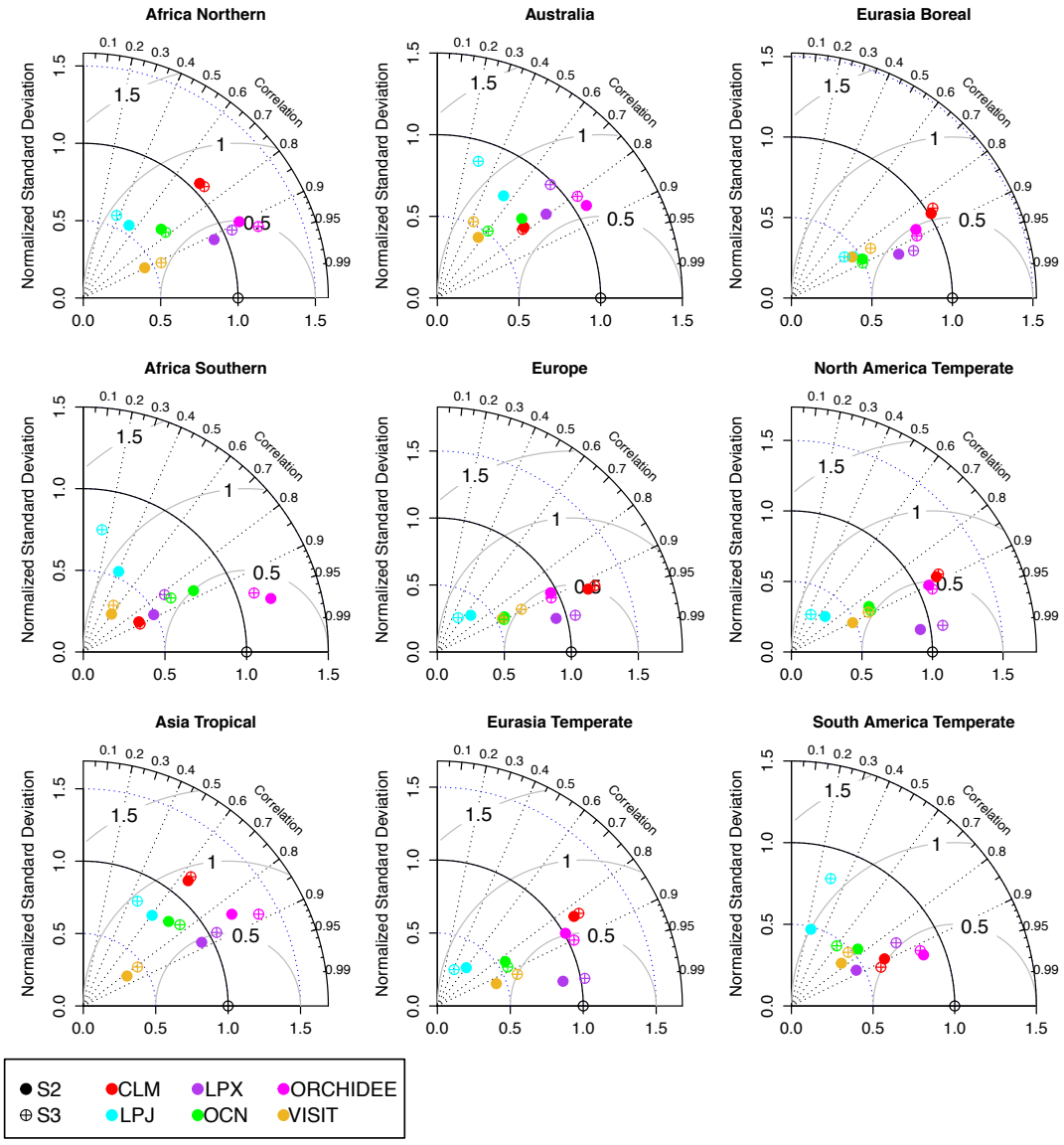

Figure S8. Europe region seasonal cycle metrics (amplitude, period, day of year (DOY) start and end) for Rise and Fall segments derived from GOSAT XCO_2 and using the segmentation analysis to extract the estimates from the 4-term mean harmonic function (pink) and the harmonic function plus interannual seasonal variation (w/ IAV). Bar plots are the median values, error bars are the minimum to maximum values for metrics; by definition, there is no IAV in the harmonic function. While the median values are similar between the two harmonic functions (excluding and including IAV), including IAV in amplitude (~1.25 ppm) and period (~25 days) will better represent model bias. A segmentation analysis will offer direct guidance via the biases in period and phase, which may differ substantially between Fall and Rise segments.

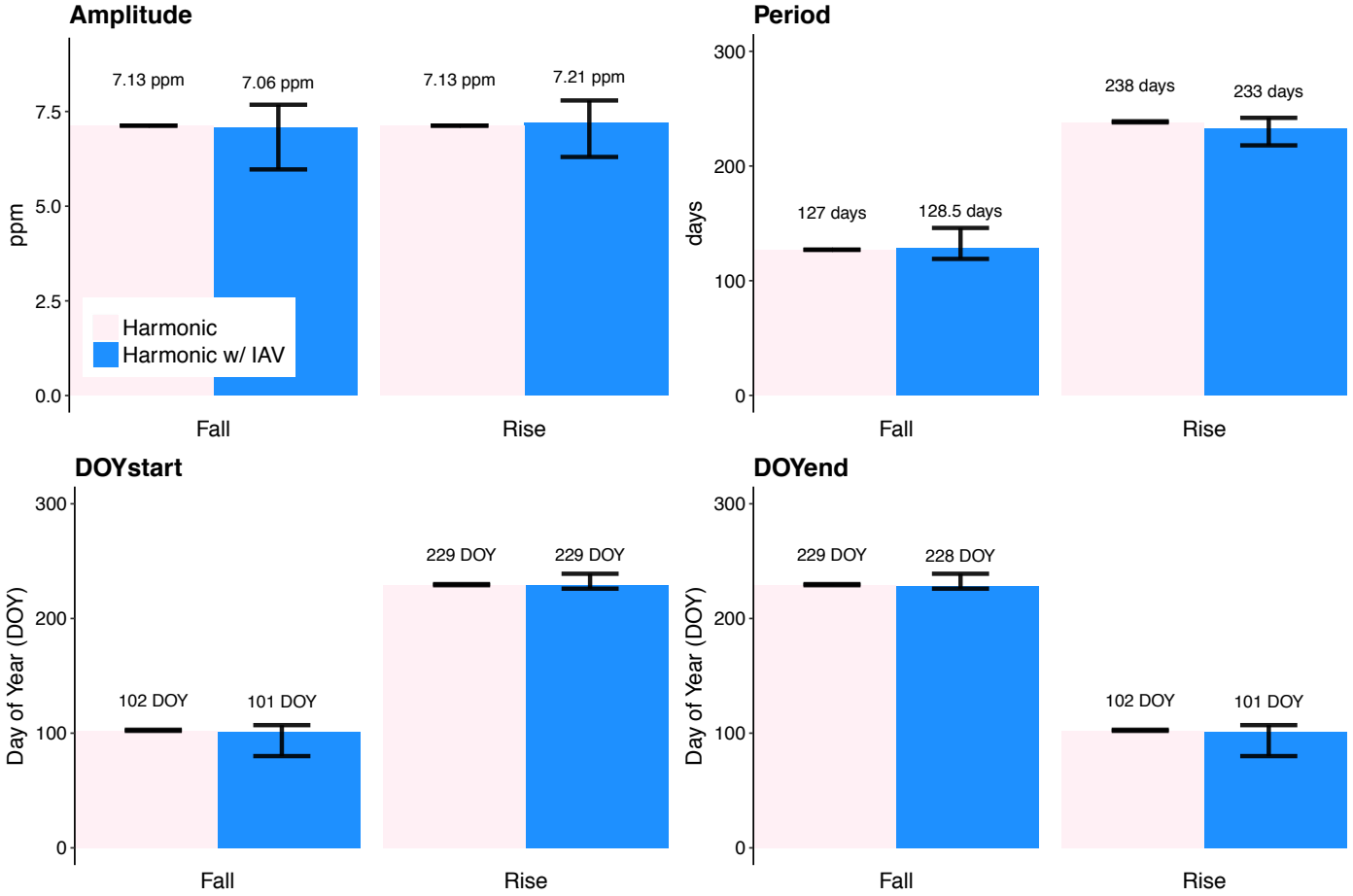

Figure S9. Long-term linear growth rates in XCO_2 (2009-2012), averaged over all TRANSCOM regions. DGVMs (x-axis) simulated the Land component of the long-term trend, and the corresponding simulations include representation of land use change fluxes.

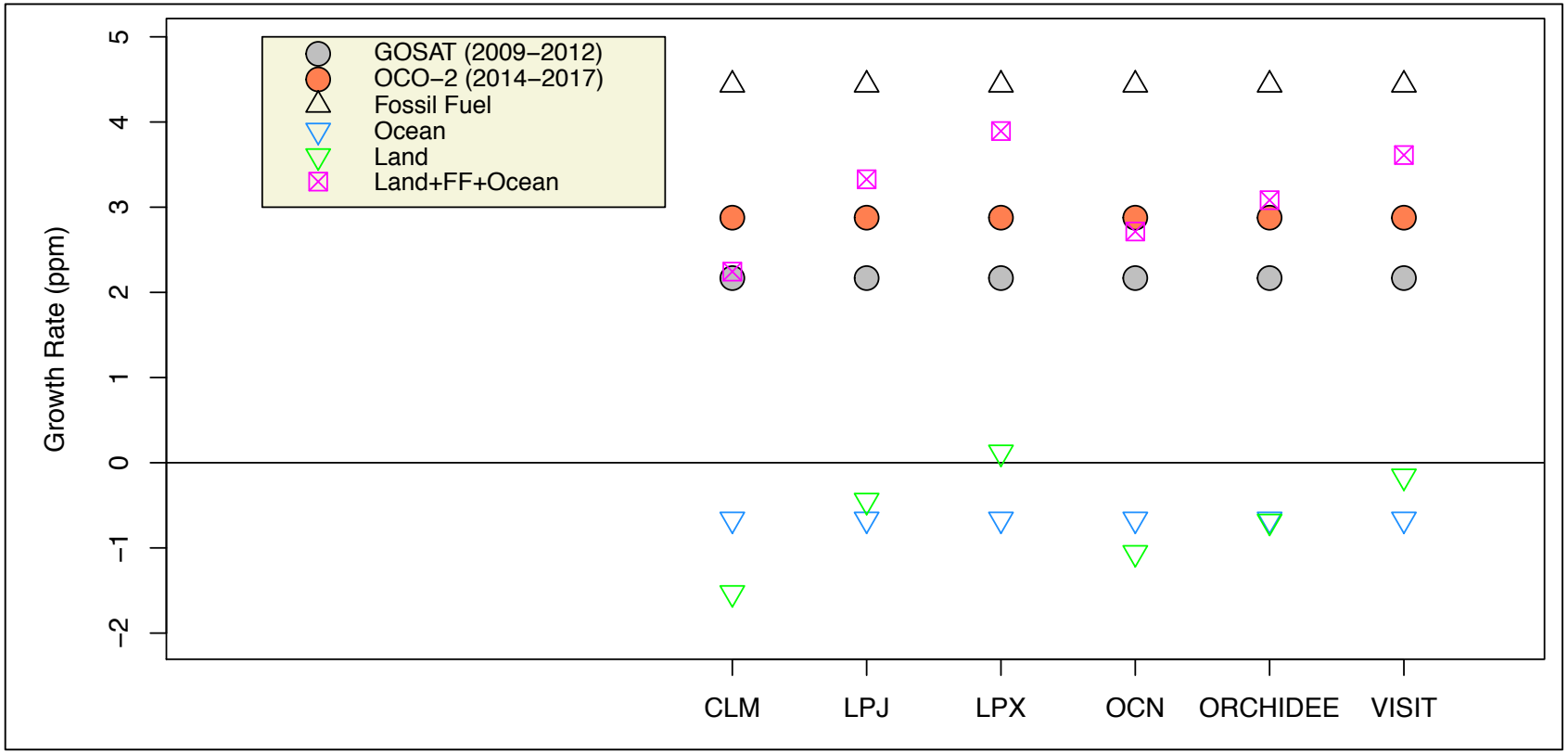

Figure S10. Correlation matrix for amplitude, period, and phase biases for Fall segments in Northern Hemisphere TransCom regions. Regression lines plotted when significant at p=0.05.

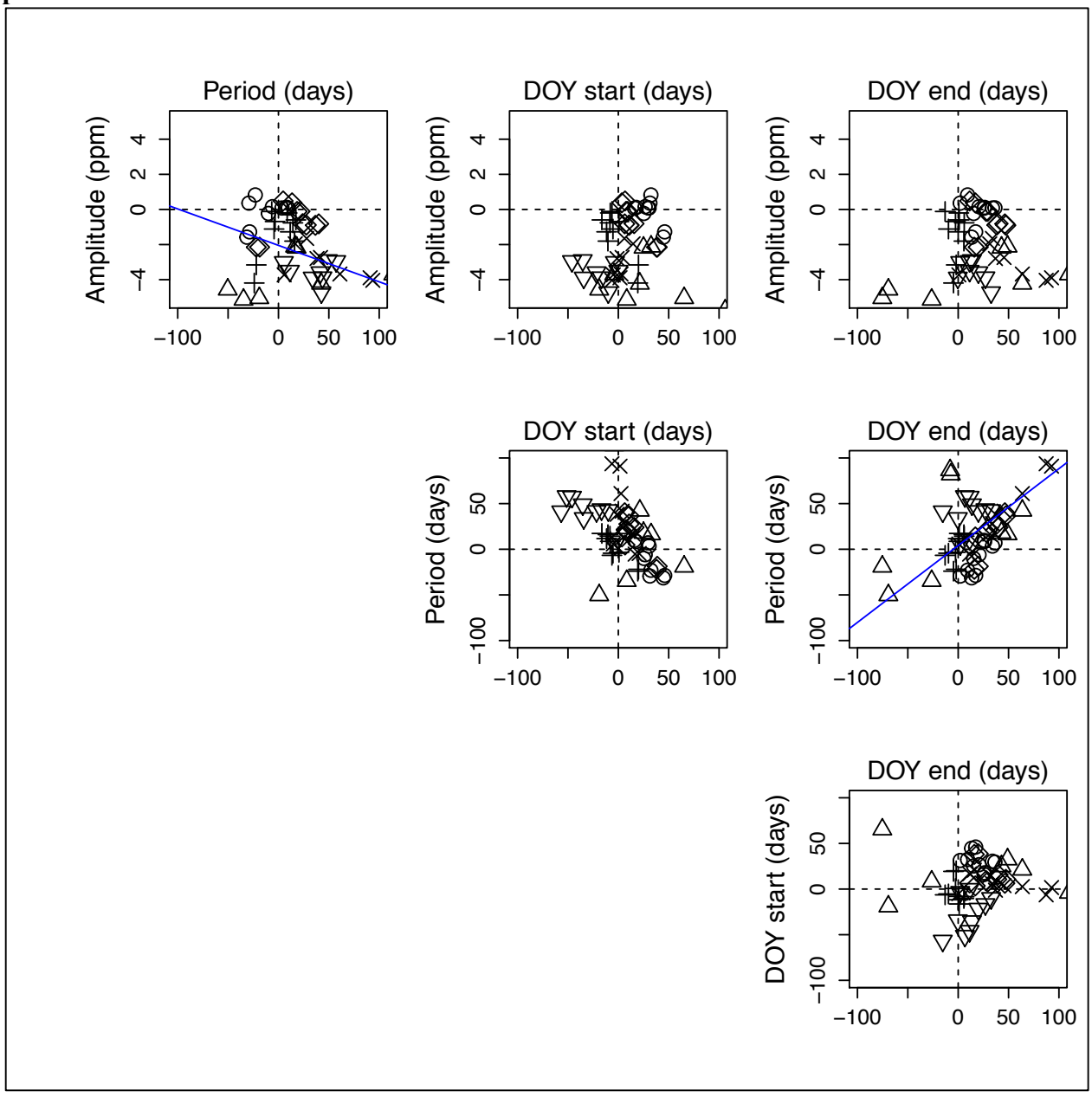

Figure S11. Correlation matrix for amplitude, period, and phase biases for Rise segments in Northern Hemisphere TransCom regions. Regression lines plotted when significant at p=0.05.

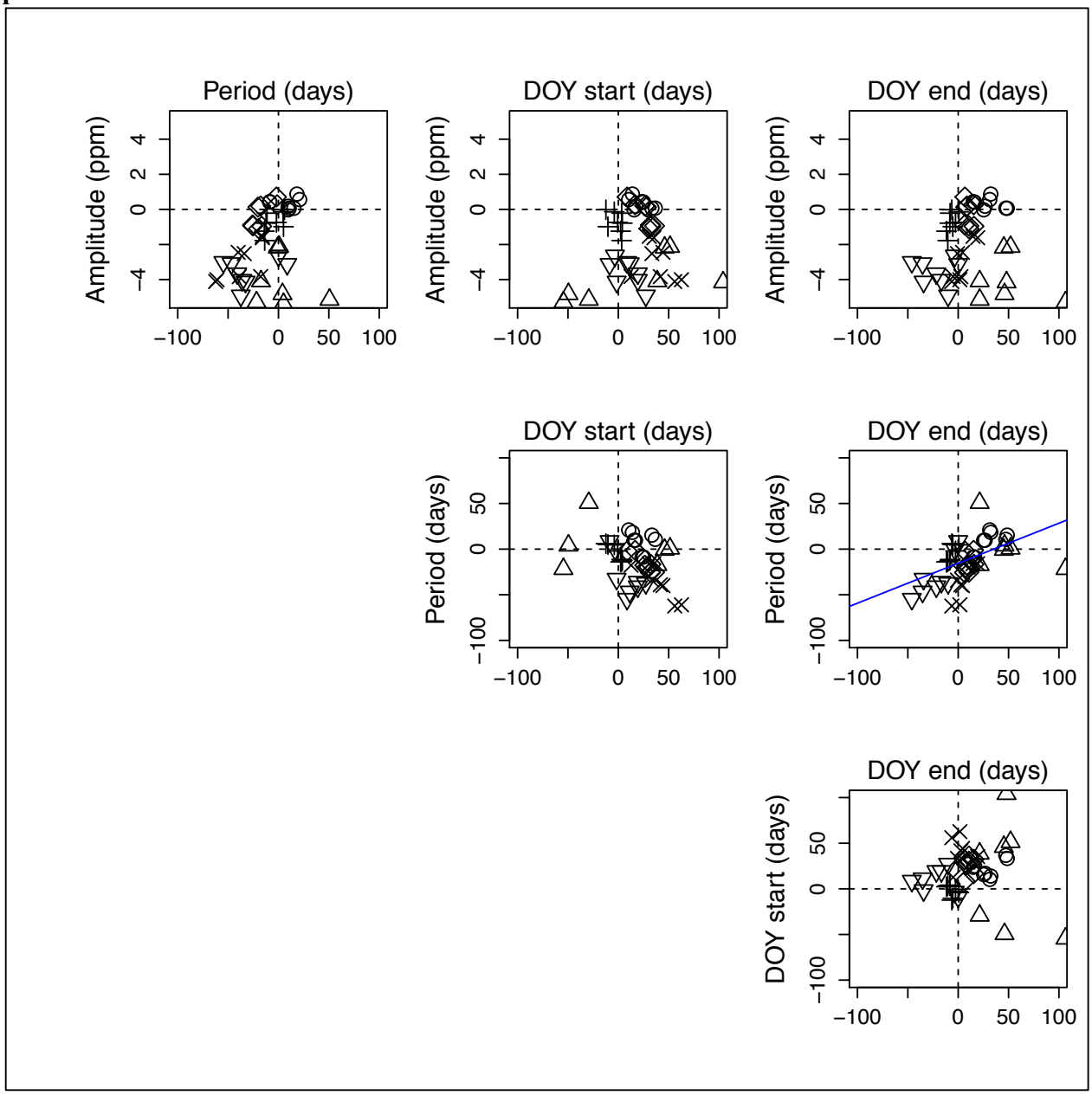

Figure S12. Correlation matrix for amplitude, period, and phase biases for Fall segments in Southern Hemisphere TransCom regions. Regression lines plotted when significant at p=0.05.

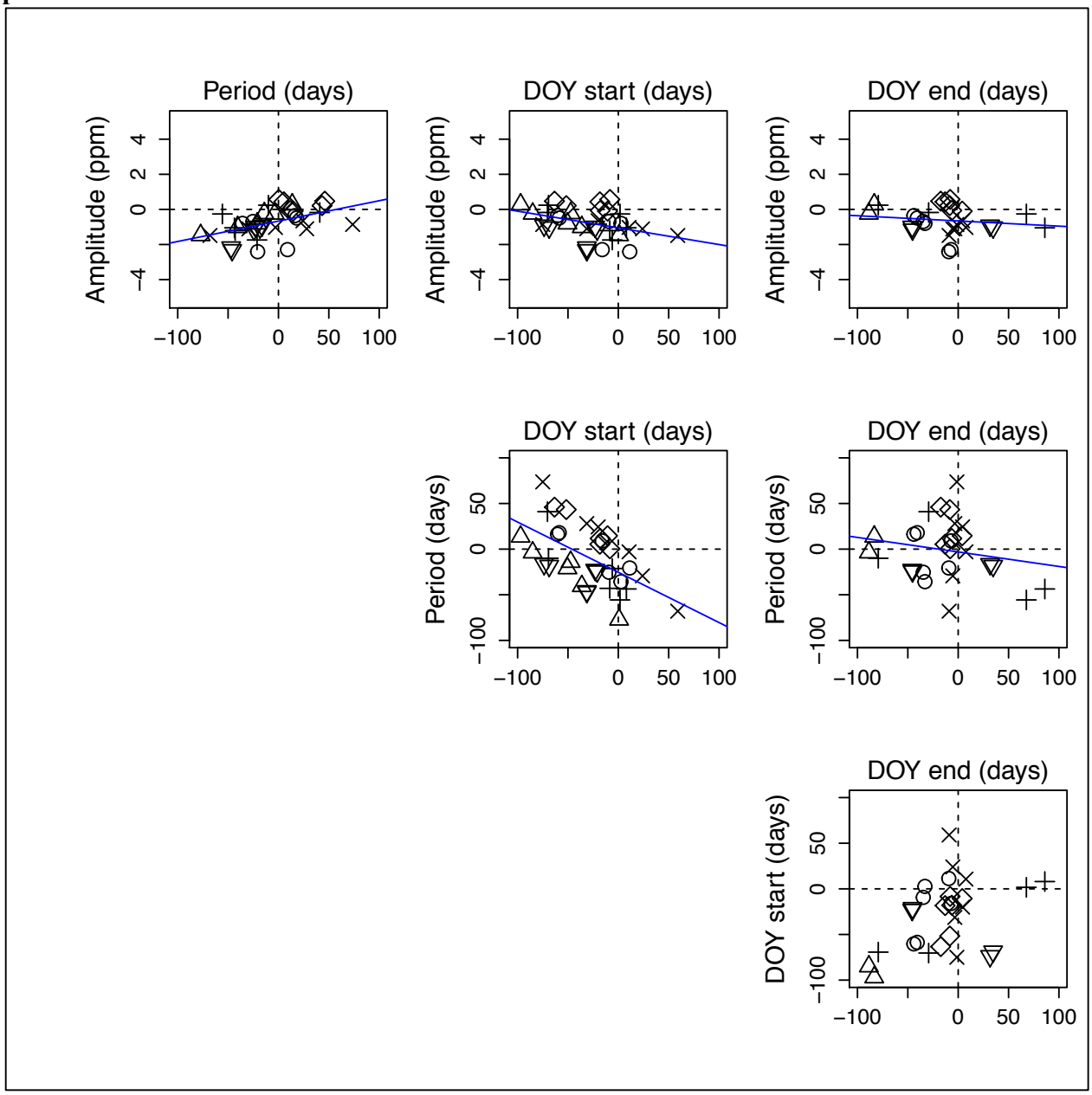

Figure S13. Correlation matrix for amplitude, period, and phase biases for Rise segments in Southern Hemisphere TransCom regions. Regression lines plotted when significant at p=0.05.